Computers in Biology and Medicine 197 (2025) 111102

Contents lists available at ScienceDirect

Computers in Biology and Medicine

journal homepage: www.elsevier.com/locate/compbiomed

Dynamic topographies of intrinsic neural timescales: a key role for consciousness

Andrea Buccellato [a,b,c,1,*], Di Zang [d,e,f,g,h,1], Yasir Çatal [c,i], Bianca Ventura [c,m], Massimiliano Facca [a,j], Zengxin Qi [d,e,f,g], Patrizia Bisiacchi [a,b], Alessandra Del Felice [a,j], Xuehai Wu [d,e,f,g], Georg Northoff [c,k,l]

[a] Padova Neuroscience Center, University of Padova, Padova, 35129, Italy
[b] Department of General Psychology, University of Padova, Padova, 35131, Italy
[c] Mind, Brain Imaging and Neuroethics Research Unit, University of Ottawa, Ontario, ON, Canada
[d] Department of Neurosurgery, Huashan Hospital, Shanghai Medical College, Fudan University, Shanghai, China
[e] National Center for Neurological Disorders, Shanghai, China
[f] Shanghai Key Laboratory of Brain Function and Restoration and Neural Regeneration, Shanghai, China
[g] State Key Laboratory of Medical Neurobiology and MOE Frontiers Center for Brain Science, School of Basic Medical Sciences and Institutes of Brain Science, Fudan University, China
[h] Department of Neurosurgery, China-Japan Friendship Hospital, Beijing, China
[i] University of Ottawa Institute of Mental Health Research, 1145 Carling Ave, Ottawa, ON, K1Z 7K4, Canada
[j] Department of Neuroscience, Section of Neurology, University of Padova, Padova, 35121, Italy
[k] Mental Health Center, Zhejiang University School of Medicine, Hangzhou, 310013, China
[l] Centre for Cognition and Brain Disorders, Hangzhou Normal University, Hangzhou, 310013, China
[m] School of Psychology, University of Ottawa, 136 Jean-Jacques Lussier, Ottawa, ON, K1N 6N5, Canada

ARTICLE INFO

Keywords:
Intrinsic neural timescales (INTs)
Consciousness
Neural dynamics
Brain topography

ABSTRACT

The brain displays intrinsic durations in its own spontaneous activity - Intrinsic Neural Timescales (INTs). INTs are hierarchically organized, with shorter durations within unimodal regions and longer intervals in multimodal domains. Despite significant progress, it's currently not known whether the unimodal-multimodal hierarchical organization undergoes recurrent changes itself - consistent with the existence of a dynamic repertoire of INT topographies. To this aim, we characterized the dynamics of topographic INT states by clustering the dynamic ACW-0 matrices in two different datasets: the source-reconstructed HCP resting-state MEG dataset, and a hd-EEG resting-state dataset, composed of healthy individuals and people with disorders of consciousness (DoCs). We found that healthy subjects display dynamic transitions between different INT states, which exhibit changing degrees of uni-transmodal cortical hierarchies. These dynamic transitions show non-random behavior, with moderate degrees of unpredictability and evidence of nontrivial memory effects. Unlike in healthy subjects, these properties are disrupted in DoC patients, who exhibit less predictable INT state transitions and less memory effects. Together, our results show a prominent role for the temporal richness of the transitions between different INT topographic states in the awake state which, as evidenced by our results, is key for maintaining an adequate level of consciousness.

1. Introduction

In the intrinsically challenging landscape of modern neuroscience, the spatial organization of neural features serves as a blueprint for computational constraints and as foundation for functional organizing principles. This topographic view of the brain, deeply rooted in neuroscience's history [1], has long guided our understanding of brain function. For instance, this view has led to the characterization of a striking feature pertaining to the brain's spatial organization: namely, that different macroscopic spatial trends display a very high degree of

* Corresponding author. Padova Neuroscience Center, University of Padova, Via Giuseppe Orus, 2, Padova, PD, 35131, Italy.
E-mail addresses: andrea.buccellato@studenti.unipd.it (A. Buccellato), wuxuehai2013@163.com (X. Wu), georg.northoff@theroyal.ca (G. Northoff).
[1] These authors contributed equally to this work

https://doi.org/10.1016/j.compbiomed.2025.111102
Received 30 June 2025; Received in revised form 4 September 2025; Accepted 13 September 2025
Available online 22 September 2025

overlap [2]. In particular, this perspective has unveiled how several cortical features (such as connectivity trends, gene expression, microcortical structures, etc …) can be placed on an almost identical continuous axis of variance - a "cortical gradient", along the continuum of a unimodal periphery and a transmodal core [3,4]. This organizational principle explains most of the variance of these spatially distributed features [5].

The brain's spontaneous activity also exhibits timescales (or durations) - Intrinsic Neural Timescales (INTs) [6,7] - which are also known to vary across cortical and subcortical networks. In fact, INTs are hierarchically distributed [8–10] (a "cortical hierarchy" can alternatively be codified as a "core-periphery" organization – see Ref. [3]) with longer timescales in multimodal, higher-order brain areas and lower durations on unimodal, lower-order areas: this has been shown in both fMRI [8,11,12] and M/EEG [3,13]. Regions with shorter intrinsic durations are highly responsive to brief, rapidly changing inputs, making them ideal for processing highly detailed and dynamic information [14]; conversely, regions with longer intrinsic durations accumulate and integrate information over extended periods, enabling more abstract and complex cognitive functions. Within this spatial model of intrinsic activity durations, information is progressively processed at increasingly longer temporal windows, which promotes an increasing degree of integration and abstraction along an uni-transmodal axis of variation [7]. Thus, the spatial arrangement of INTs further exemplifies the role of cortical topography as a fundamental organizational principle of the brain, shaping cognitive processes across various domains (see Ref. [7] for a review). However, limited knowledge exists regarding the temporal variability of INTs and whether their uni-transmodal topographic spatial distribution across the cortical surface varies over time. While glimpses into the dynamic nature of INTs have emerged [15], how INT topography evolves over time remains a gap in the current scientific inquiry.

As a matter of fact, cortical topography itself can undergo either spontaneous or task-driven transitory rearrangements. A notable example can be found in functional connectivity (FC) studies where, through the application of dimensionality reduction algorithms, such as the k-means algorithm [16] (see also [17]) - which partitions dynamic functional connectivity (dFC) matrices into spatial clusters - it has been revealed that resting-state networks (RSNs) [18] undergo continuous reorganization, even at short timescales [17,19–23]. Further, this dynamic view of brain topography is not specific to RSNs and has been recently extended to several other spatiotemporal features of the brain's activity, leading to the current notion of "dynamic brain states" [24]: a series of "spatially distributed patterns", which are explored by the brain in a non-trivial manner, reflecting its capacity to process information efficiently [25]. This leads to understanding cortical topographies as underlying factors of global modes of information processing - and their relevance to brain functioning and consciousness [17].

Following this line of reasoning leads to the question of whether INTs undergo a similar set of topographic rearrangements as a function of time. Does the brain display a repertoire of dynamic topographies of INTs, and are richer transition dynamics relevant for consciousness? Our investigation followed a dual strategy. Initially, we utilized MEG resting-state recordings from healthy subjects (HC) from the open access Human Connectome Project dataset [26] to validate the approach proposed in this study; more specifically, we aimed at determining whether clustering algorithms could reveal spontaneous dynamic reorganization over time in the topographic organization of INTs across the cortex of healthy fully awake subjects. In fact, the use of source-reconstructed MEG data offers the opportunity of enhanced spatial resolution, enabling a comparison of the dynamic INT states' topographic properties with established maps from unrelated studies but indexed in the same coordinate space. This allowed us to explore the dynamic properties of the time series describing the transition between dynamic INT topographies.

Secondly, we employed a high-density EEG (256 channels) dataset, which included both healthy conscious subjects and individuals with disorders of consciousness (DoC) [27]. DoCs are clinical states characterized by reduced or total loss of consciousness and are due to severe acquired brain injuries; while its taxonomy is still debated [28,29], it can be roughly described with two main diagnostic categories: the unresponsive wakefulness syndrome (UWS) [30], which is characterized by regular eyes opening but with no overt signs of consciousness, and the minimally conscious state (MCS) [31], a less severe condition, which is instead characterized by evidence of diminished, but fluctuating behavioral responsiveness. In this second step, we investigated whether disruptions of the dynamic features of the cortical topography of INTs were consistent with disruptions of healthy conscious behavior.

This type of investigation may have the benefit of substantiating even further the link between the brain's topographic features and its own intrinsic set of coordinates, laying the theoretical basis for a crucial principle of brain function: although previous research has shown that INT topographies follow a core-periphery organization [6], it is plausible that these spatial patterns dynamically reconfigure in response to environmental demands. This relationship between the dynamic features of INTs and its topographic organization also has very important implication for consciousness, as posited by the Temporospatial Theory of Consciousness (TTC) [32,33]. TTC is a theory of consciousness that starts with the assumption that the brain "constructs" its own intrinsic spatial and temporal features, and that the way these spontaneous and intrinsic features of neural activity relate to the external environment are key to consciousness; based on this assumption, TTC aims to fill a gap between neural and mental features of consciousness and proposes four different neural mechanisms which map consciousness onto four different dimensions. In TTC, it is suggested that a rich "repertoire" of timescales forms the basis of healthier consciousness levels and a richer phenomenology [7,33], which gives further theoretical ground to exploring the topographic dynamics of INTs as an innovative opportunity to characterize consciousness.

2. Results

2.1. MEG: basic topographic features of INT state properties

The time series data representing the dynamic evolution of intrinsic timescales topography in the MEG resting-state recordings was subjected to k-means clustering. K-means clustering was used for the purpose of segmenting INT topographies into distinct recurring spatial patterns, identifying the most representative topographic states over time (further details in Methods section 4.7). Both of the optimization criteria we employed resulted in the identification of an optimal solution of four clusters (k = 4) (Fig. 1b), and this solution was selected for further analysis. The four resulting maps, corresponding to distinct intrinsic timescale topographies (or INT states), are displayed in Fig. 1a; the correlation matrix representing the pairwise correlation between each map is presented in Supplementary Fig. 2.

A qualitative attribute which is already discernible through visual inspection is that most of these maps seem to display a cortical gradient: shorter INTs are usually represented in more peripheral regions, which suggests the presence of the well-known [3] hierarchical spatial organization of INTs. Each state's average coverage (%) [34] is shown in Supplementary Fig. 2a and in Supplementary Table 2.

Does this qualitative observation carry any topographic significance? In order to test whether these maps followed a core-periphery organization, we divided the parcels into the 12-networks organization described in the Methods section. A core-periphery ratio (C/P ratio) index was obtained by dividing the average INT duration of the kth map's core regions by the duration of the periphery regions: the higher the C/P ratio, the more the core-periphery organization is assumed to be prominent. Results are displayed in Fig. 2. This did indeed yield different degrees of core-periphery gradients in the four topographic INT states. As the C/P ratio indexes the distance between INT lengths in core regions and peripheral (unimodal) regions, it also quantifies how

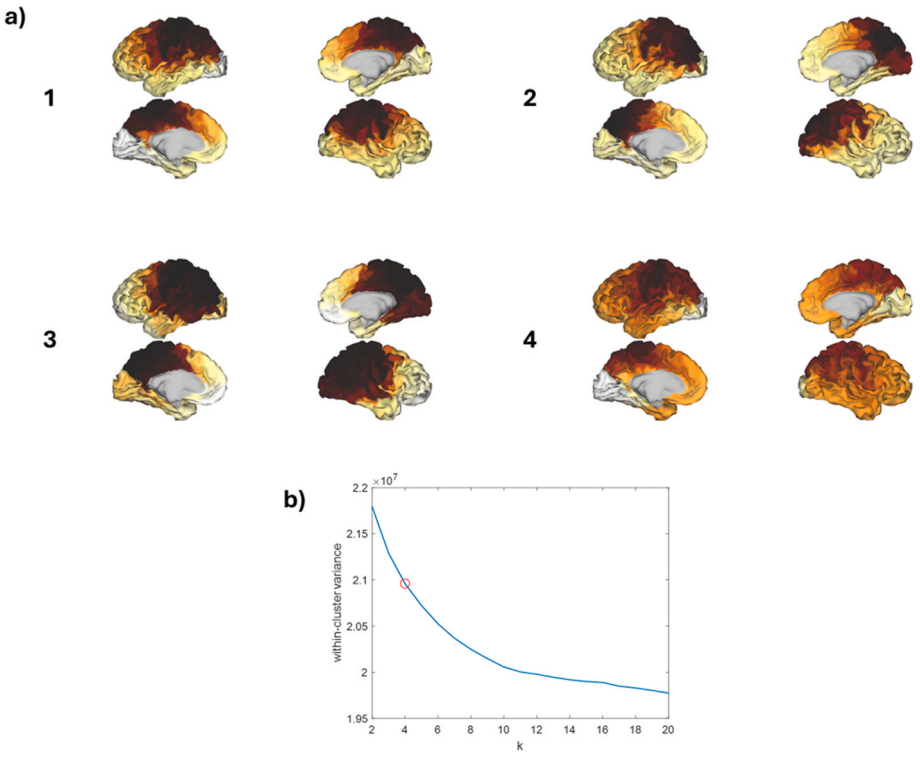

Fig. 1. MEG topographic plots of the four maps describing the repertoire of observable INT states, obtained with k-means clustering. a) INT states, which we define as the recurrent topographic patterns of INTs found after clustering the dynamic ACW-0 matrices, are here depicted and numbered orderly from one to four. These states are not ranked according to any arbitrary principle, and therefore the number assigned to each state does not identify them with any particular property: however, we will refer to particular states by referring to our (arbitrary) number assignment. Colormap is organized as following: darker colors identify higher INT durations; in brighter colors, lower values INT values; very light coloring indicates very low INT values. INT values range are here shown in relative percentages, representing the relative magnitude of the INT lengths after data is normalized. b) the within-cluster variance vs k graph, which illustrates the optimization criterion used in this study to select the best number of INT states. The optimal k is here shown as the knee point of the graph (k = 4, indicated by a red circle), which represents the point after which there is lower decrease in the variance across clusters than with lower ks. (For interpretation of the references to color in this figure legend, the reader is referred to the Web version of this article.)

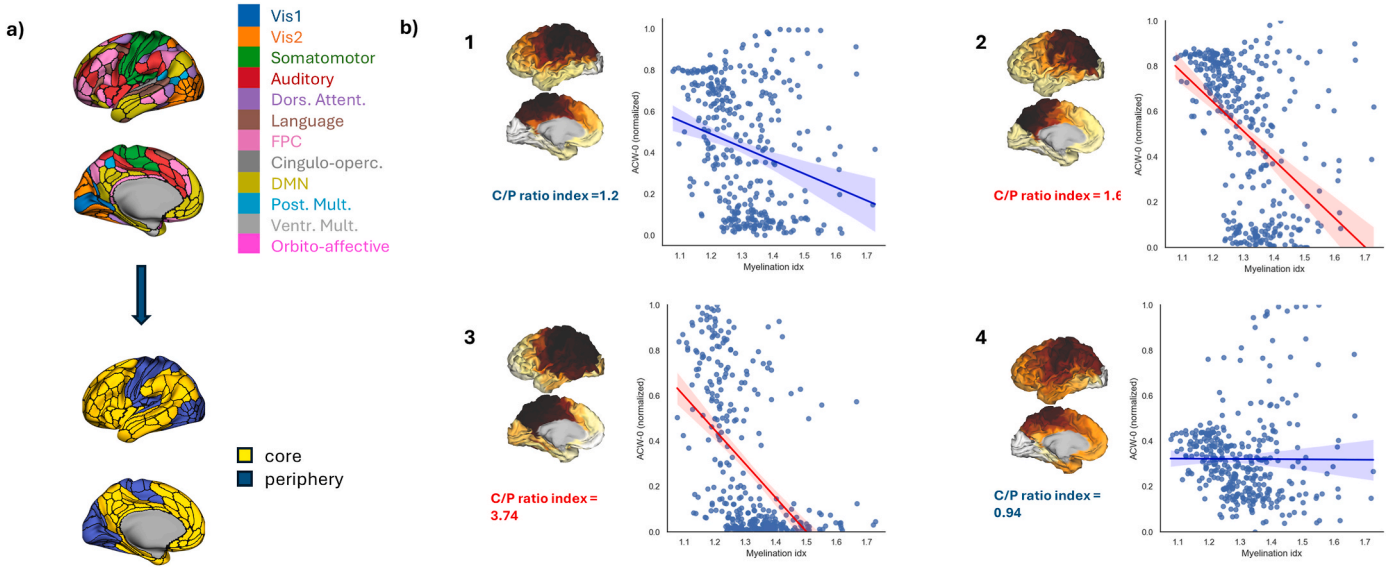

Fig. 2. Uni-transmodal or Core-periphery organization and spatial hierarchy of the 4 INT state maps (in MEG). a) For each map, a 12-networks parcellation scheme (upper figure) was applied, averaging INT lengths over parcels belonging to the same network; a legend is provided to interpret the colormap used in this figure. Each network was consequently labeled as belonging to either core or periphery (bottom figure) as described in the Methods section. b) For each INT state map, we show: its C/P ratio index, which is here defined as the ratio between the average of the core regions INT values and the periphery ones; a scatter plot depicting the spatial correlation between the full, parcel-level INT state map and the myelination index map. In red, we highlighted maps which displayed a significant correlation after a spatial permutation test (spin-test). Spatial correlation coefficients and their respective p-values after correction are reported in Table 1. (For interpretation of the references to color in this figure legend, the reader is referred to the Web version of this article.)

relatively "short" the peripheral regions' INTs are with respect to higher-level regions. We observed C/P ratios higher than 1 in almost all maps, which indicates shorter INTs in peripheral regions, in line with previous findings.

To further substantiate the presence of cortical hierarchy in these INT states, we spatially correlated each map with a myelination index map (T1w/T2w ratio). The degree of myelination follows a cortical hierarchy, with lower myelination in higher-order areas and higher myelination in lower-order areas. Here, we use it as a proxy to assess the hierarchical organization of our four INT states. Hence, higher or lower correlation values between INT states and myelination do not imply that INT values become independent or strictly dependent of myelin, but rather indexes whether INT topographies follow a cortical hierarchical gradient. Scatter plots depicting the pairwise spatial correlation for each state can be found in Fig. 2b.

All maps correlated negatively with the myelination index map. Among the 4 INT state maps, two maps (maps 2 and 3) passed the spatial permutation statistical test ("spin-test", Methods section 4.13): statistical significances and their relative spatial correlation indices are shown in Table 1. These findings are coherent with a dynamic perspective on INTs undergoing spontaneous reorganization with rearrangements of their topographical distribution as a function of time.

Furthermore, a linear relation between the degree of cortical hierarchy and the C/P ratio arises (Fig. 2b): the higher the degree of hierarchy in the state under examination, the longer (on average) the intrinsic timescales of that state in the core regions.

Together, we observed a hierarchical organization of INTs - in line with recent findings [3,9,35,36] - while we also extended these findings by showing dynamic transitions among different INT topographic states.

2.2. MEG: statistical properties of dynamic INT state transitions

The primary objective of this section is to ascertain the statistical properties of the time series describing the dynamic transitions between distinct INT states (an example of such time series can be found in Supplementary Fig. 1a). We started by testing whether these time series were the outcome of random processes by employing a runs test (see Methods section 4.9). A runs test assesses the randomness of a sequence by evaluating the occurrence and distribution of consecutive similar values, thus detecting non-random patterns in data. The rejection of the null hypothesis of randomness across all subjects and their respective recordings provided compelling evidence for the presence of a non-random process governing the observed topographic INT transitions.

Further, we show that the average time spent in a state (using pairwise within subject correlation with 30 windows in state 2, 15 in state 1, etc …) is on average fairly high ($r_{12} = 0.71$; $r_{13} = 0.60$; $r_{23} = 0.72$) across all three resting-state recordings. This suggests that the relative percentage of time spent in the exploration of these states is considerably stable within subjects across their different recordings.

A sequence of state transitions can be modeled as a Markov process (see Methods section 4.10). A crucial feature of a Markov process is its empirical transition (also known as "syntax") matrix, which indexes the probability of visiting, starting from a *k*th state, any given *k* state. The average transition matrix of the HCP dataset (Supplementary Fig. 1b) reveals that self-transitions are more likely to occur on average than transitions between different states. This suggests that transitions occur on a longer timescale than the sliding window overlap size (90 % overlap) with a certain stability over time. However, while we can still observe that often self-transitions have a higher likelihood, a great deal of heterogeneity can be observed when comparing syntax matrices across different individuals (Supplementary Fig. 1c); this, instead, suggests that there are significant inter-individual differences in how the dynamics of transitioning between state unfold as a function of time.

From the transition matrix, one can also verify the memory properties of the system by testing against the properties of 0^{th} and 1st order Markovianity [34]. The null hypothesis of testing against 0^{th} order Markovianity states that the probability of transitioning to a state is not influenced by information about the previous state. In all subjects, across all recording sessions, this null hypothesis was rejected, indicating a certain degree of memory of the state transitions time series data. On the other hand, the null hypothesis against 1st order Markovianity states that information about the current state is not influenced by past states further than one. This hypothesis was rejected for forty-four MEG recordings (Supplementary Table 3), suggesting that in these recordings, memory could extend even beyond 1st order Markov properties.

Having assessed the statistical properties of the transitions between INT topographies, we also investigated the amount of temporal information contained in these time series. To this end, we computed the complexity of this categorial time series data on the full MEG sample with the Context-Tree Weighting algorithm (Methods 4.11). Average sample values (mean = 0.67; std = 0.30) were obtained. A non-parametric bootstrap test showed that the observed CTW values did not arise as a result of chance (mean = 0.88, $p < 0.001$). Moreover, surrogate data testing based on the Iterative Amplitude Adjusted Fourier Transform algorithm (Supplementary Methods 1.2) confirmed this finding: test CTW values were significantly lower than those observed in the surrogate-based INT state transition time series ($p < 0.001$). Reinforcing further prior observations about the intra-subject stability of INT state estimation across different recordings, no significant differences were found between within subject CTW values across the three different resting-state sessions (in order, from first to third: mean = 0.64, std = 0.19; mean = 0.68, std = 0.23; mean = 0.71, std = 0.21; $\eta^2 = 0.006$) (Fig. 3c). An additional analysis which consisted in computing the INT state transition's Sample Entropy (SampEn) (m = 3, tau = 1) confirmed the aforementioned findings (Supplementary Results 2.3).

Lastly, the memory properties of the transitions between INT states were probed. A system which displays memory properties may display a degree of self-association which decays exponentially as a function of increasing time lags. If that applies, one can estimate the degree of memory by fitting an exponential curve to the function describing its self-dependency. One can then extract the decay rate parameter of the resulting fit: a lower decay rate corresponds to a longer temporal reach on the influence of a perturbation on the examined system – i.e. "more memory" – and vice versa. The procedure in order to estimate these properties of the transitions between INT states is described in Fig. 3. Similarly to CTW, the decay rate of the Auto-Cramer's function (Fig. 3d) did not change significantly across the three available resting-state (in order, from first to third: mean = 0.41, std = 0.13; mean = 0.41, std = 0.11; mean = 0.43, std = 0.11; $\eta^2 = 0.003$).

Table 1
Spatial correlations between the kth INT topographic states and the myelination index in MEG. In bold, the map number and their respective correlation values that resulted significant after testing for significance. p-values are obtained after a permutation "spin-test" and Holm-Bonferroni corrected for multiple comparisons.

k	p-value (spin test)	Pearson's R
1	>0.05	−0.2496
2	**<0.01**	**−0.4722**
3	**<0.01**	**−0.5332**
4	>0.05	−0.0052

2.3. EEG: basic topographic features of dynamic INT states

Here, we investigated whether the temporal richness of INT states exploration decayed along with loss of consciousness in people with DoC, as predicted by TTC. [7,32,33]. To test for this hypothesis, we applied the same procedure on a hd-EEG dataset consisting of DoC individuals.

In concordance to what we observed MEG, the procedure applied to

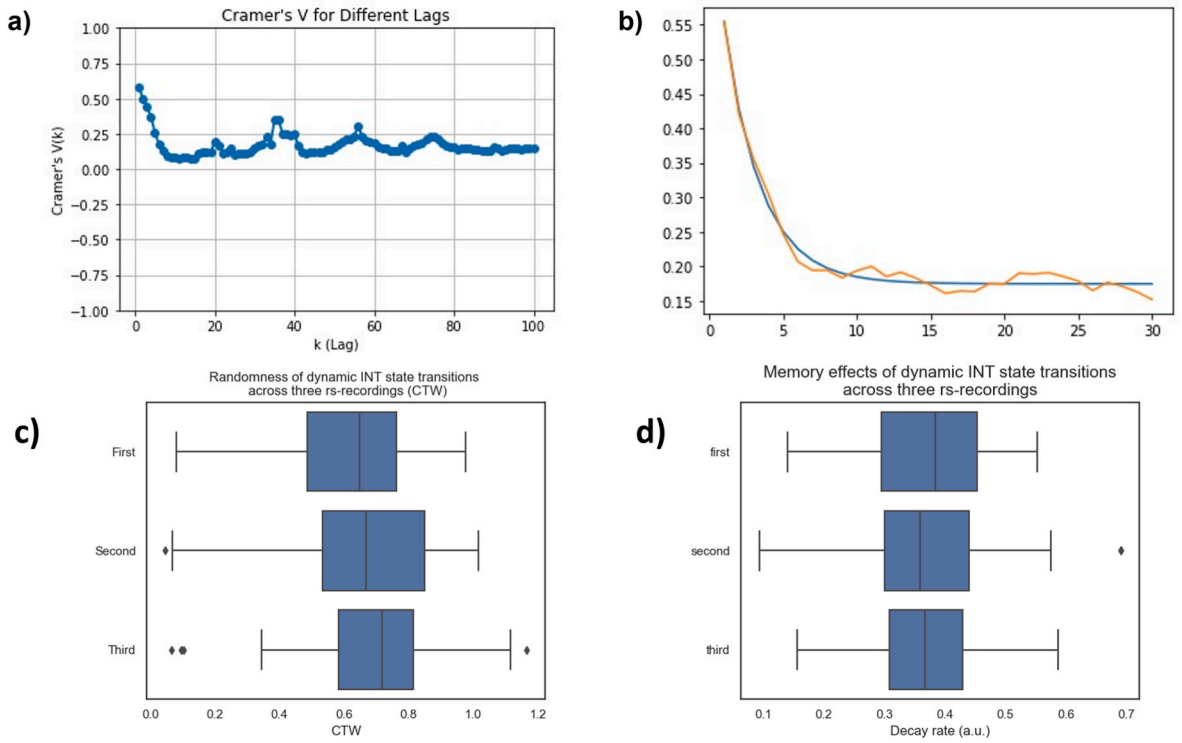

Fig. 3. Intra-subject consistency across different recordings of the unpredictability and the memory properties of INT state transitions. a) Auto-Cramer's function of an individual subject, for visualization purposes. Cramer's V is computed for the INT state transition time series with a delayed copy of itself at increasing k lags, similarly to what is done to obtain a signal's autocorrelation function. In the first part of the Auto-Cramer's function, one can recognize an exponential decay, indicating memory properties in the time series. b) For the same subject, we show: the Auto-Cramer's function, for the first 30 lags (in orange); the exponential decay fit (in blue). The resulting estimated exponent indicate how fast a certain process loses memory of its past states. c) Boxplots depicting the change in the unpredictability of the transitions between INT states (indexed by CTW), across three different recording sessions. No change in the group average values and in the distribution shapes were detected. d) Similarly to what is observed in c), no significant change in the mean values and distibution shapes could be detected for the groups' decay rate values of the Auto-Cramer's function across the three recording sessions. (For interpretation of the references to color in this figure legend, the reader is referred to the Web version of this article.)

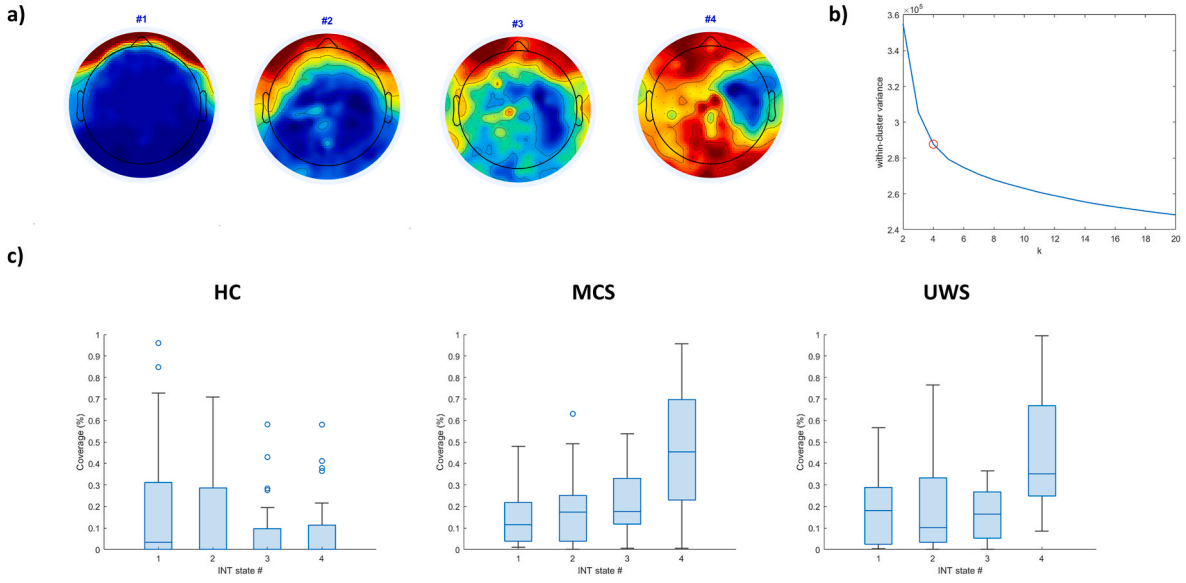

Fig. 4. EEG topographic plots of the four states describing the repertoire of observable INT states, obtained with k-means clustering. a) Similarly to what we have presented in Fig. 1, we do not present these states with any form of ranking. Colormap is organized as following: in red, longer INT lengths; in blue, lower INT lengths; yellow tints indicate intermediate values. INT values range from 0 to 1, as data is normalized before clustering. b) Both optimization criteria indicated an optimal number of $k = 4$ maps (indexed by a red circle in the figure) c) Group-specific INT states coverage (presented as a relative percentage) for each map. (For interpretation of the references to color in this figure legend, the reader is referred to the Web version of this article.)

the EEG sample resulted in an optimal number of k = 4 maps describing the variability of the topographic data (Fig. 4); as both optimization criteria resulted in the selection of 4 maps, this was selected for further analysis. The maps are shown in Fig. 4a.

Regarding group differences in the time spent in each INT state (Fig. 4c), healthy subjects explored on average state 1 and 2 more frequently: both states correspond qualitatively with the same spatial gradient which is appreciable in "static" ACW topographies [37] and in our MEG data too. On the other hand, both DoC populations spent a significantly larger amount of time exploring state 4, which instead seems to represent a less hierarchical and more "homogenous" INT topography. A chi-square test between each group's state coverage reveals significant differences for all states in the pairwise comparison between HC and both UWS and MCS populations ($p < 0.05$), while revealing no appreciable difference between DoC populations. Mean coverage values are shown in Supplementary Table 1.

2.4. EEG: abnormal statistical properties of the transitions between INT topographies in disorders of consciousness

Is the disruption of INT state transition dynamics associated with loss of consciousness? To address this question, we assessed the statistical properties of the INT states time series, separately for our three EEG groups.

As already shown in the MEG dataset, the null hypothesis of randomness (via the runs test) was rejected for all HC state transitions. Unexpectedly, this applied as well to the UWS and MCS group, indicating that, when consciousness is lost to different degrees, the transitions between topographic INT states preserves a certain degree of non-randomness, differently to what is expected from an entirely random process.

Similarly to MEG, we tested the INT state transition time series data against 0^{th} and 1st order Markovianity, starting from the obtained transition matrices. In the HC population, all 0^{th} order test were rejected for all recordings, as expected; moreover, all null hypotheses were also rejected for both DoC groups. This indicates that, even when consciousness is lost, a certain degree of memory is still preserved in the dynamics of INT state transition process. Regarding 1st order Markovianity, the null hypothesis was rejected for almost all HC subjects (Supplementary Table 4), which confirms that in healthy conscious conditions memory extends past beyond the immediate previous INT topography. Surprisingly, in seven MCS and four UWS subjects (Supplementary Table 4), the null hypothesis was rejected.

In the next step, we compared the complexity values extracted from the INT state transitions of both conscious and unconscious groups, by computing CTW (Fig. 5a). A non-parametric statistical test indicated that populations differed significantly ($p < 0.05$; mean HC = 0.67, std HC = 0.31; mean DoC = 0.78, std DoC = 0.26; $p < 0.05$; $\eta^2 = 0.5$). Holm-Bonferroni-corrected pairwise post-hoc comparisons (Supplementary Fig. 4a) revealed a significant difference between the HC and the UWS group (mean UWS = 0.83, std UWS = 0.32; $p < 0.01$, $z = -2.4$) but not between the HC and the MCS group (mean MCS = 0.78, std MCS = 0.26; $p > 0.05$, $z = -1.4$), and the UWS and MCS groups ($p > 0.05$, $z = 1$). When grouping both DoC populations, their pairwise comparison with healthy controls remained significant ($p < 0.05$, $z = -2.3$). Overall, the two DoC groups showed significantly higher CTW values when compared to healthy conscious subjects, which is consistent with a more random exploration of INT topographies over time. A multiple comparison corrected confirmatory analysis, using the SampEn (m = 3, tau = 1) entropy estimator, further substantiated these findings (Supplementary Results 2.3 and Supp Fig. 5a and Fig. 6a).

This is further confirmed by that bootstrapping temporally shuffled INT state transitions yielded a very highly disordered behavior (mean CTW = 0.89), significantly different from the observed empirical average mean values (for all groups, $p < 0.001$). Similarly to our findings in the MEG sample, we also applied a surrogate test (based on the IAAFT algorithm, Supplementary Methods 1.2): the HC population CTW values remained significantly lower than the surrogates ($p < 0.001$), while interestingly enough, the surrogate test on the DoC sample did not result in significantly different CTW values ($p > 0.05$).

Additionally, to test whether the unpredictability of INT state transitions predicted the behavioral responsiveness of DoC patients, we correlated the obtained CTW and SampEn values with the corresponding CRS-R scores: this did not result in a significant correlation for both measures ($p > 0.05$).

Regarding the memory properties of the transitions between INT states, we found significant differences in the three groups' decay rates (mean HC = 0.30; mean UWS = 0.39; mean MCS = 0.36; $p < 0.05$, $\eta^2 = 0.12$). The HC sample displayed a lower decay rate estimate on average. Post-hoc comparisons showed significant differences only between the HC and the UWS population ($p < 0.05$, $z = -2.1$), but not between HC and MCS ($p > 0.05$, $z = -1.1$) and UWS vs MCS ($p > 0.05$, $z = 1.3$) (Supp. Fig. 6b). Resulting p-values were Holm-Bonferroni corrected. When grouping UWS and MCS as a single DoC population, the difference remained significant (Fig. 5b, $p < 0.01$, $z = -2.7$).

We conducted a series of control analyses to assess the potential influence of alpha oscillations and aperiodic activity on our findings for both samples (Supplementary Methods 1.1, 1.5, and 1.6). As shown in Supplementary Results 2.2, 2.4, and 2.5, while both components appear to contribute to some degree, there is no indication that they solely drive the observed effects, either in terms of topographic patterns or temporal dynamics. Specifically, we observed a moderate correlation between EEG alpha power and map #4 (rho = 0.52) and a weaker negative correlation for the FOOOF aperiodic exponent with map #3 (rho =

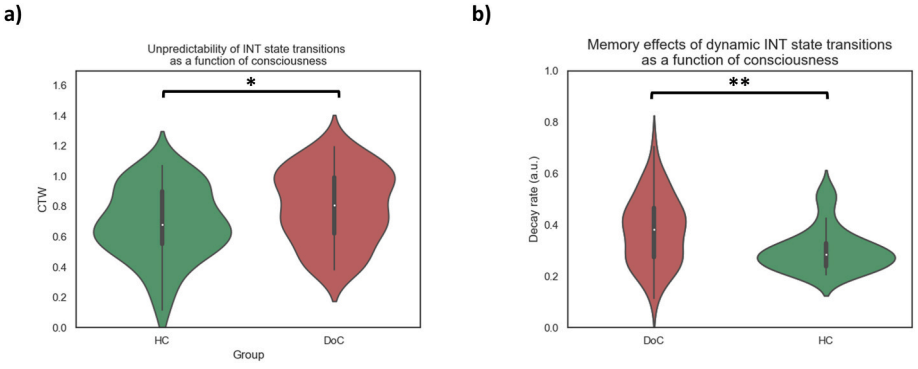

Fig. 5. Randomness and memory effects of the dynamic INT transition time series as a function of different states of consciousness. a) Violin plots depicting the subject-wise average CTW values of the dynamic INT transition time series in healthy wakeful consciousness (HC), compared the DoC population. In all violin plots, * indicates $p < 0.05$, ** indicates $p < 0.01$ and *** indicates $p < 0.001$. The absence of any sign stands for non-significance ($p > 0.05$). b) Violin plots depicting the subject-wise average decay rate of the exponential fit to the dynamic INT transition time series in healthy wakeful consciousness (HC), compared to DoC.

−0.31), indicating that these spectral features have only a modest relationship with INT topographies.

3. Discussion

We investigated the brain's spontaneous topography of Intrinsic Neural Timescales (INTs) and its dynamic behavior, modeled as a series of transitions between different scalp INT distributions. Our methodological strategy involved the estimation of INT dynamics, by using the well-known Autocorrelation Window – 0 (ACW-0) with a windowed approach, with the consequent use of a k-means clustering algorithm to partition the data into a k set of topographic INT maps. A graphical abstract, which synthetize the methods and findings of this study is provided in the text.

The novelty of this approach demanded special attention, especially regarding the validity of the methodology applied. Clustering algorithms are a very popular choice in neuroimaging studies, which most popularly led to a whole area of investigation: microstates analysis [38]. However, to our knowledge, the dynamics of INT topography have not been investigated yet with such methods. The goal of the first section of this study was therefore to assess that clustering methodologies can identify appropriate topographic characteristics of INTs.

3.1. INT dynamics and topographic transitions

It is established that one of INT's most remarkable features is its hierarchical organization on the cortical surface [3,9,11]. This peculiar spatial organization, which can also be expressed as a "core-periphery" topography [3], is known to support hierarchical processing of the temporal information contained in the incoming inputs, from shorter durations typically processed in unimodal regions to longer durations that are processed in higher-level, multimodal areas. Here, we show that two of the four INT states obtained on the HCP MEG resting-state dataset follow a significant hierarchical organization; this was done by spatially correlating each INT state to a myelination index map [39], which was used as a proxy to quantifying an "index" of cortical hierarchy - as in Ref. [40–42]. The correlation matrix displayed in the Supplementary Fig. 2b, together with the varying correlations with the myelination map, confirms that the INT state maps exhibit distinct spatial distributions. Indeed, a significant amount of spatial correlation can be observed between these different maps; this is a finding that is coherent with the functional significance of a core-periphery topography. Therefore, this seems to indicate that INT maps maintain a core organization while transiently shifting in their spatial distributions, rather than undergoing a complete reorganization. We also show that the degree of hierarchical organization goes hand in hand with a core-periphery organization [3]: the higher the hierarchy "index", the more pronounced the distance between core and periphery regions.

Additionally, as measuring INT lengths ultimately relies on calculating the neural signal's autocorrelation function – which is known to be tightly related to its spectrum [43], INT map topography might be influenced by well-known spectral properties such as the total power in the alpha (8–13 Hz) range and the aperiodic spectrum exponent [44]. As these factors—namely, posterior alpha power and the aperiodic exponent—may causally influence the observed INT state maps, we performed several additional analyses to investigate their potential contributions. A first approach involved measuring the map similarity between the topographic maps of alpha power and the aperiodic exponent and the INT state maps in both MEG and EEG datasets (Supplementary Methods 1.2 and 1.3). The results, reported in Supplementary Results 2.2, revealed only modest associations, expect for: a moderate correlation between the aperiodic exponent and map #4 in the EEG sample, likely reflecting the marked homogeneous topography of this INT state map - with longer INT values in posterior regions, typically seen in lower states of consciousness (Fig. 4); a moderate correlation between the EEG alpha power topography and map #4. We interpret the discrepancies between MEG and EEG as reflecting methodological limitations in EEG source localization, which may reduce the ability of INT maps to capture fine-grained hierarchical patterns. Additionally, to corroborate these findings, map similarities were computed using Euclidean and cosine distance as a similarity index, instead of Pearson's r (Supplementary Methods 1.2). Findings did not differ significantly, except for a significant correlation of both scalp distributions with INT state #4 (Supplementary Tables 9 and 10).

A complementary approach tested the robustness of our findings by controlling for potential confounding signal components. Alpha oscillations were removed by notch-filtering around each subject's individual alpha frequency (IAF), and the full analysis was repeated (see Supplementary Methods 1.7). The resulting INT state maps and dynamics remained largely consistent with original findings, despite some differences in optimal state numbers and transition entropy values findings (Supplementary Results 2.4). Additionally, we controlled for aperiodic EEG components by estimating INTs directly from power spectral density, which showed significant topographical similarity to ACW-0 derived maps (Supplementary Results 2.5).

Taken together, these findings suggest that although spectral measures may contribute to INT topography and contribute with meaningful information, their influence appears relatively modest and do not point to strong confounding effects, indicating that spectral properties of the neural signal do not solely account for the observed spatiotemporal patterns, corroborating the robustness of our findings. Nonetheless, the possibility of partial confounding cannot be entirely excluded, and this issue will require more systematic investigation in future studies.

3.2. The relevance of non-random INT state transitions

Assessing the temporal statistics of spontaneous transitions between different INT topographies unveiled the presence of a non-trivial dynamic behavior in the topographic organization of INTs in a healthy conscious population, display significant memory effects and a moderate degree of unpredictability, as shown collectively by the violation of Markov properties, and our CTW and Sample Entropy (SampEn) results. We therefore suggest that our findings show the dynamic transition between the different INT topographies is not generated by a random process, therefore carrying a significant degree of information.

First, violations of 0^{th}-order Markovianity is interpreted as evidence that transitions between INT topographies follow a nontrivial structure, rather than occurring as random, memoryless sequences.

In this study, CTW served as an estimator of the entropy rate of the INT state transition time series, capturing the degree of randomness in the sequence of state changes, while SampEn quantified the regularity of repeated temporal patterns within the same series. In both cases, higher values indicated more unpredictable, random-like transitions, whereas lower values reflected more stereotypical and deterministic sequences. Within the context of INT state dynamics, we interpret intermediate values of both metrics as reflecting a repertoire of transitions that balances stability with flexibility—suggesting a functionally advantageous regime for adaptive neural processing, generally implying a balance between prediction and chance in the INT topographic state transitions [45]. SampEn and CTW values do not necessarily converge, which further suggests that INT state transitions are both more irregular (SampEn) and display more randomness in INT state-to-state evolution (CTW) in DoCs. While we acknowledge that SampEn and CTW may target different aspects of temporal complexity, the qualitative similarity of the findings obtained here results in the interchangeable use of the terms "complexity" and "entropy" when referring to the unpredictability of INT state transitions.

The effects of randomness on CTW values can be observed by temporally shuffling the state transition time series, with CTW approaching its higher limit, as we observed here. Further, our surrogate analyses underscore the nuanced interpretation of CTW. Temporal shuffling produced highly disordered dynamics, significantly above

empirical values in all group, confirming meaningful temporal structure. Contrary to expectations. the IAAFT test yielded significantly higher complexity in healthy individuals but no significant differences in DoC patients. This pattern suggests that while HC signals preserve structured dynamics, the already disordered repertoire in DoC limits the sensitivity of surrogate testing. Moreover, because IAAFT preserves autocorrelation and power spectra while scrambling phases, it may normalize the signal by removing nonstationary components, thereby affecting clustering outcomes. We suggest that further evidence is needed to clarify the interpretation of complexity metrics in future works, with longer recordings and individual-level clustering, which we argue will be essential to disentangle the roles of entropy, nonstationarity, and repertoire richness.

The decay rate of categorical autocorrelation is interpreted as an index of how long past INT states continue to influence future transitions, with slower decay reflecting greater temporal memory in the system. These findings complement the analysis on Markovian properties, attempting a quantification of INT state transitions memory properties.

Overall, these results suggest that the spontaneous exploration of different INT topographies is underpinned by a non-random dynamic process. The consistency of these findings across different recording sessions further substantiates the coherence of the approach.

What is the computational advantage that a spontaneous rearrangement of the spatial organization of INTs could confer to the way the brain processes the temporal information of incoming inputs?

Although our results provide evidence for the dynamic behavior of the cortical arrangement of INT values, it is actually plausible that this topography undergoes multiple rearrangements: if the process underlying these INT state maps is indeed dynamic and functionally significant, merely replicating a static hierarchical organization would be of limited value—particularly considering the brain's need to swiftly adapt to the evolving temporal statistics of its environment. In line with this view, recent work has shown that cortical timescale gradients themselves can dynamically shift, not only in their local topography but also through non-local interactions between regions [46]. We therefore suggest that adapting to the temporal statistics of the environment requires not only intraregional modulation of INTs but also relatively rapid changes in their hierarchical organization, supporting a moderately complex repertoire of INT states.

Remarkably, both optimization criteria supported an optimal number of 4 INT states in both modalities (MEG and EEG). Interestingly, this corresponds to the number of microstates consistently identified across the literature (Bréchet and Michel, 2022; [38]). Microstate analysis is a well-established approach for characterizing "global patterns of scalp potential topographies" and their dynamics ([38]; Rubega et al., 2024), and are thought to reflect instantaneous interactions between networks (Koenig et al., 2002) which can also predict cortical connectivity patterns (Abreu et al., 2021). Given the direct relation between connectivity and INTs ([11,47]; Ryan V Raut et al., 2020), a link between microstates and INTs is plausible - though highly speculative at this stage - and warrants direct investigation in future studies.

3.3. Relevance of INT state transitions for consciousness

One main finding of this work is that the dynamics of INT states deteriorate as consciousness is lost, as posited by the Temporo-spatial Theory of Consciousness (TTC) [32,33]. Additional validation of our findings were corroborated by a stability analysis across bootstrapped subsets of both datasets (see Supplementary Results 2.7).

Within the theoretical framework of TTC, the brain's dynamic features— and most notably for the present study, the spontaneous fluctuations of intrinsic neural timescales—are fundamental to understanding consciousness [32,33]. Furthermore, the way these timescales are spatially distributed across the cortex is critical for processing temporal information from incoming stimuli [6,33]. Importantly, our results reveal that the temporal aspects (INTs) and the spatial aspects (cortical topography) converge in this study, highlighting their combined role in underpinning conscious experience, which is coherent with other studies [48]. As a matter of fact, in TTC it is argued that an adequately complex repertoire of timescales should enhance the flexibility of this temporal input processing mechanisms [7], promoting more flexible and adaptive neural dynamics which, in turn, underpin higher levels of consciousness and a richer phenomenological experience. Our findings provide empirical support for this idea.

We demonstrate that INT state transitions are produced by non-random processes, even in the absence of behavioral consciousness signs. Furthermore, 1st order Markovianity often inadequately models INT state transitions in healthy subjects, suggesting high memory extending beyond immediate past states. The relevance of INT state dynamics extends beyond TTC predictions, aligning with Integrated Information Theory (IIT) [49] and the Entropic Brain Hypothesis [50]. Both theories emphasize complex neural dynamics as consciousness hallmarks: a richer yet structured "dynamic repertoire" of INT states may enhance brain sensitivity to temporal environmental information, consistent with the Entropic Brain framework. We propose that the flexibility provided by dynamic INT states reveals correspondence between the cause-effect structure underlying consciousness's physical substrate and phenomenological properties of temporal experience.

Surprisingly, a subset of patients in both DoC groups displayed INT dynamics—such as 1st-order Markovianity of state transitions—closely resembling those observed in healthy individuals, despite the overall group differences. This suggests that our approach may capture clinically relevant heterogeneity within the DoC population, beyond the coarse distinction from healthy awake subjects. Here, we did not observe a significant correlation between the unpredictability of INT state transitions and CRS-R scores; however, this should not be interpreted as conclusive evidence against its relevance for assessing consciousness. The null result may reflect limitations in our current characterization of INT dynamics or the known variability and constraints of behavioral assessments like the CRS-R [51], which may not fully capture underlying neural processes [28]. Importantly, previous studies have shown that entropy-based measures of neural complexity and unpredictability can differentiate levels of consciousness [52]. While our approach focuses specifically on the temporal evolution and repertoire of INT states rather than raw signal complexity, the general trend aligns with the notion that more complex or less predictable neural activity corresponds to higher levels of consciousness. Supporting this, supplementary analyses (Supplementary Fig. 11) show that average SampEn values in the EEG sample are generally lower in DoC patients compared to healthy controls. Taken together, these findings tentatively suggest that INT state transitions may provide a neurophysiological index of consciousness at the individual level, even in the absence of behavioral responsiveness [53,54]. Future studies—particularly in conditions with a clearer ground truth, such as sleep or anesthesia [55]—will be essential to validate these observations and explore their correspondence with other neurophysiological markers of awareness.

We show that loss of consciousness is accompanied by increased randomness in INT state transitions, as reflected by entropy-based measures (CTW, SampEn), and by a faster decay of temporal memory in state dynamics. Since INTs are thought to index the brain's capacity to process temporal information [6,56], and their topography shapes computational modes, these findings suggest that when both unpredictability and temporal dependence in transitions are disrupted, the system loses the structured dynamics required to sustain meaningful neural representations of the environment. In this sense, the conceptual mapping of randomness, memory, and Markovianity converge on the view that consciousness depends on maintaining a balanced repertoire of structured yet flexible state transitions (see Fig. 6 for a very schematic depiction of this notion). Therefore, our results provide first-hand evidence of predictions arising from the Temporo-spatial theory of consciousness (TTC): richer INT dynamics in conscious individuals, with

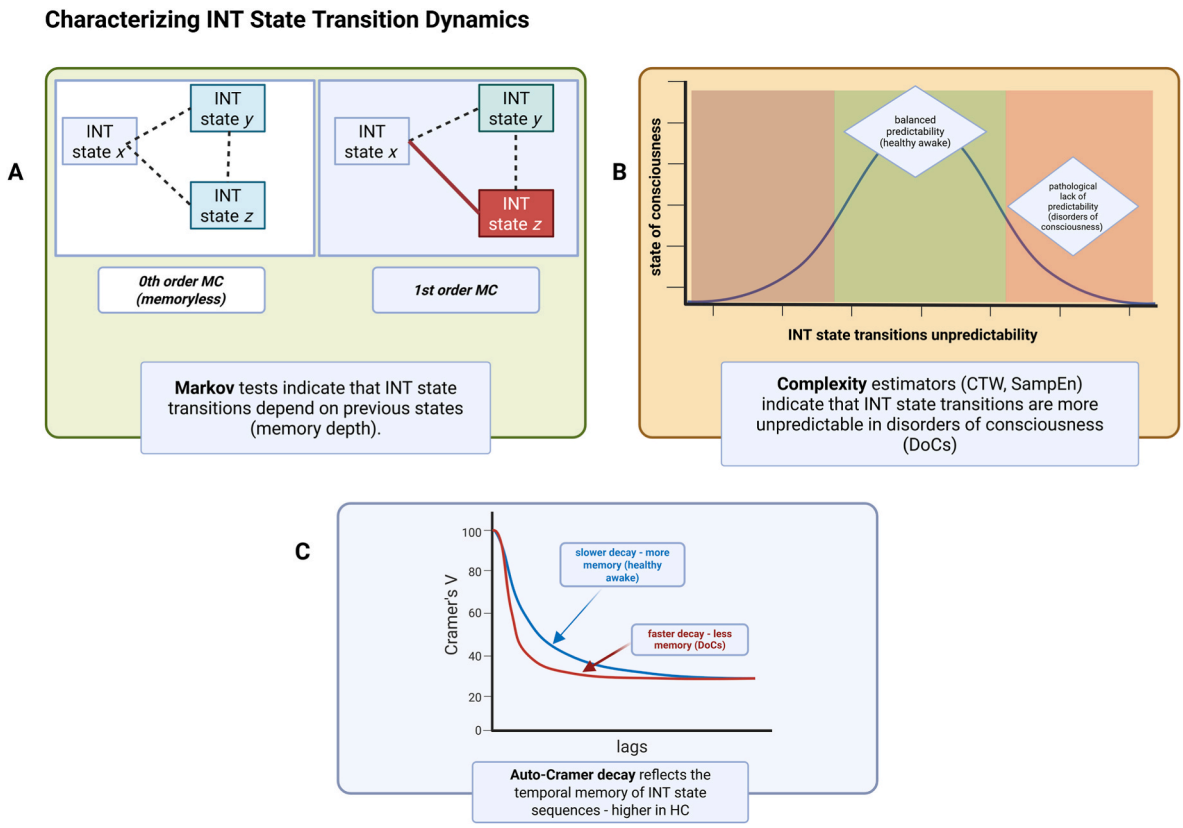

Fig. 6. Correspondence between INT state transition dynamics and their functional interpretation. A) Schematic illustration of 0th-order (memoryless) and 1st-order (memory-dependent) Markov Chains (MC) used to model INT state transitions. Statistical tests indicate that transitions, in the majority of our samples, depend on the previous state, consistent with 1st-order Markovianity (often even extending to states further than the current – see Results and Supplementary Tables 3-4), which is here depicted schematically as higher likelihood (in red) of transitioning to a certain state, depending on the current state (INT state x, in our example). Here, this is interpreted as a consequence of a certain nontrivial degree of structure in the transitions between INT topographies. B) Entropy-based estimators (CTW, SampEn) quantify the unpredictability of INT state transitions. Healthy wakefulness is associated with an intermediate, balanced level of unpredictability, whereas disorders of consciousness (DoC) show pathological increased unpredictability. We argue that a higher unpredictable sequence of INT state transitions underlines a lower capability of adapting to the temporal structure of the perceptual environment, which in turn hinders healthy levels/states of consciousness. C) Temporal memory of INT state sequences was assessed via the decay of categorical autocorrelation (Cramer's V) across time lags. Healthy controls (HC) show slower decay, reflecting greater memory in state dynamics, while DoC patients show faster decay, indicating reduced temporal dependence. Complementary to the results on the Markovianity of INT state transitions, this metric attempts to quantify the degree of memory contained in the categorical time series data which represent the dynamics of the cortical topography of INTs. (For interpretation of the references to color in this figure legend, the reader is referred to the Web version of this article.)

respect to reduced or absent consciousness states.

3.4. Future directions and limitations

The scope of this study is restricted to resting-state data. Future research will need to be centered on the mechanisms that generate the observed dynamic behavior of INT states: insights might be gained from applying similar analytical methods to task-based data, or from computational models in which parameters—such as connectivity or intracolumnar excitatory/inhibitory balances—are systematically manipulated.

Spectral properties of the M/EEG signal, including alpha power and the aperiodic exponent, could potentially influence INT topography. However, our control analyses indicate that, although a modest influence cannot be entirely ruled out, these measures did not significantly contribute to the observed INT dynamics (see Supplementary Methods 1.1 and Results 2.2).

Arguably, a methodological limitation of this study is related to the use of sliding window analysis to track the temporal changes of ACW-0 values (dACW-0), as several concerns have been raised against the use of this technique in functional connectivity studies [57,58]. In the case of dFC studies, while there are many factors that might be confounded for genuine FC changes from window to window, the main concern seems to be related to sampling errors. In the case of our dACW-0 analysis, we chose this simple but limited approach because of the novelty of this hypothesis, as a windowed analysis does not require any modeling of the underlying dynamics which remain unknown to this day. Further, we mitigated the sampling error effect by using relatively large sized windows (8 s), as detailed in the Methods section. However, limitations inherent to this method can only be addressed by either applying different methods, such as statistical autoregressive models [59], or by future studies that take advantage of the temporal structure of an experimental task to test whether the changes in dACW-0 time series match behavioral state changes.

Likewise, we employed a k-means clustering algorithm guided by the same parsimony principle that led to the use of sliding windows. There are two main problems with this unsupervised learning algorithm, which stem from the same constraint: the number of clusters is decided a priori by the experimenter. Because of that, a first issue is that the algorithm will always find clusters for which there is no guarantee of their actual significance, while the second issue is related to the choice of k (the number of clusters), which can be either be guided by visual inspection or by using more strict criteria. For instance, in microstates analysis, it is indicated to use a meta-criterion (a "democratic" voting

based on the collective scoring of other criteria) [38] to select the optimal number of clusters, but in our study we decided to use only two criteria to improve the interpretability of our results – including the pitfalls of our methodology. We suggest two alternatives that can potentially improve the validity of the present study in future studies. First, it will be important to test whether comparable dynamic INT states emerge when applying alternative dimensionality reduction techniques, such as principal component analysis, independent component analysis, or related approaches; alternatively, through the use of simulated data, where the ground truth is known, one can also test for the sensitivity of the k-means algorithm to truly detect the spatiotemporal configurations that are theoretically explorable by the brain.

A key limitation of the present work is that the EEG analysis was conducted in sensor space rather than source space. Source reconstruction in patients with disorders of consciousness is particularly challenging and potentially unreliable, as structural brain lesions alter conductivity properties and can substantially bias localization accuracy [60]. Furthermore, the use of template head models in place of individual anatomical data introduces additional uncertainties that limit the interpretability of EEG source-level results [61]. For these reasons, and in line with prior studies in this population, we restricted the EEG analyses to sensor space. Moreover, because our EEG analyses were restricted to sensor space, there is no direct correspondence between scalp electrodes and cortical hierarchy maps which, together with the substantial inter- and intra-subject variability in electrode placement, undermines interpretability when attempting to align sensor-level activity with canonical gradients. For these reasons, we did not perform a direct comparison in the EEG sample. We warrant future investigations in healthy participants, where reliable source reconstructions and standardized electrode-to-cortex mappings can be applied. For similar reasons, we also acknowledge that no quantitative comparison between EEG- and MEG-derived INT states was performed across modalities, which would require within-subject multimodal datasets in healthy participants. Nonetheless, the EEG and MEG states showed a convergent pattern of antero–posterior prominence, supporting the interpretability of the EEG findings despite the absence of direct source-level mapping.

Additionally, the clustering procedure was applied to concatenated group data, treating groups as a whole, and not on single subjects. We adopted a group-level clustering approach for three main reasons: (i) concatenating across subjects increases the number of windows and thereby improves clustering accuracy given the limited recording length (~5 min per subject); (ii) it enables direct group-level comparisons of INT dynamics; and (iii) it provides common topographies that facilitate comparison with MEG-derived states and standard maps. Since concatenating data is likely to produce "false transitions" [62], we argue that individual-level clustering represents an important avenue for future research; recent work (reliability Liu) also highlights promising approaches for bridging group- and individual-level dynamics, which could further strengthen interpretability in this context.

3.4.1. Conclusion

We investigate the brain's dynamic topography of Intrinsic Neural Timescales (INTs) in two different modalities (MEG and EEG). Our findings show evidence of non-random dynamic transitions between different topographic INT states, derived from applying a k-means clustering procedure on a sliding windows ACW-0 analysis. Source reconstructed MEG data confirmed that at least a good percentage of the dynamic INT states are consistent with an uni-transmodal or core-periphery organization, but also reveals a new set of non-hierarchical INT topographies. Importantly, the dynamics of INT topographic state transitions can be characterized by non-randomness, temporal predictability, and long-range memory. Together, these findings demonstrate a rich repertoire of INT topographies changes in the fully awake state.

Applying the same analysis in a hd-EEG dataset consisting of people with disorders of consciousness (DoC), we found that the dynamic transitions between INT states are nonrandom in these subjects. However, their loss of consciousness is associated with lower long-range memory and increased unpredictability, implying poorer INT topographic dynamics. Together, albeit indirectly, these findings point to the importance of the INT state dynamics for maintaining the level/state of consciousness. These results provide direct evidence for the Temporospatial Theory of Consciousness (TTC), which postulates richer dynamic INT repertoires in conscious states and convergence of temporal and spatial dynamics in contributing to a higher level of consciousness.

4. Methods and materials

4.1. MEG data acquisition and experimental details

The open access resting-state (rs) magnetoencephalogram (MEG) data from the Human Connectome Project (HCP) repository was used in the first section of this study [26,63,64]. The MEG system includes 248 SQUID sensors.

The dataset used in this study consisted of 84 subject in the age range of 22–35 years, each subject undergoing three consecutive resting-state recordings of the same length. During each of the 5 min resting-state scans, subjects were instructed to lie, with eyes open, while a fixation cross was presented on a screen. Further details about the subject population demographics and the acquisition parameters can be found in Ref. [63].

4.2. MEG preprocessing

MEG data were preprocessed using the standard HCP pipeline (rmegpreproc stage) [63]. In brief, recordings were band-pass and notch filtered, channels and time points with artifacts were identified and rejected, and independent component analysis (ICA) was applied to remove ocular and cardiac artifacts. Differently from the standard HCP pipeline, bad segments were identified on z-scored amplitude, and flatline channels/muscle artifacts were linearly interpolated to minimize discontinuities. Full details are reported in the Supplementary Methods (Supplementary Methods 1.1).

4.3. Source reconstruction

Source reconstruction followed the HCP icamne stage, applying weighted minimum norm estimation (wMNE) to project independent components into a source space of 8004 cortical vertices. Data were then parcellated into 360 HCP-MMP atlas regions [65] and grouped into 12 large-scale functional networks [11]. For analyses of core-periphery organization, sensorimotor and early sensory networks were defined as periphery, and higher-order networks as core. Full methodological details are available in Supplementary Methods 1.1.

4.4. EEG data acquisition and experimental details

Eighty-one individuals with DoC ($n_{UWS} = 39$; $n_{MCS} = 42$; mean age = 46.65 ± 15.89 years old; M/F sex-ratio = 2.24; etiology: stroke = 43; anoxia = 7; traumatic brain injury = 31) were recorded in resting state—at bedside—for 5 min using a Geodesics system (Ges300, EGI, Eugene, OR, USA) and a 256-channel electrode cap (HydroCel 130, EGI, Eugene, OR, USA) (following 10–20 international systems). Standard systematic procedures, such as the Arousal Facilitation Protocol [66], were followed to ensure high wakefulness and arousal levels in the participants undergoing the recording session. To avoid interference related to medication, examiners did not administer any sedative agents in the 24-h period that preceded the recording session. The clinical assessment was performed on admission, through the Glasgow Coma Scale (GCS) [67], while the differential diagnosis was carried by trained clinicians by repeatedly applying the JFK Coma Recovery Scale–Revised (CRS-R) [66], selecting the best total score over all assessments. Additionally, a control sample of 44 healthy controls (HC) (age 31.3 ± 16.1

years, M/F sex-ratio = 0.94) underwent a 5-min resting-state hd-EEG recording session, recorded with the same 256-channel system (GES 300, Electrical Geodesics, Inc., USA). Healthy participants were asked to lie on the bed and keep their eyes open to mirror the EEG recording of the DoC sample. EEG data were re-referenced online to Cz and acquired at a sampling rate of 1000 Hz, while the impedance of all electrodes was kept to less than 20 KΩ. Further details about the datasets used in this study can be found in Ref. [37].

4.5. EEG pre-processing

EEG preprocessing was performed with EEGLAB [68] and custom MATLAB scripts. Data were resampled, band-pass filtered (0.5–40 Hz), and noisy channels were identified, interpolated, and re-referenced to the common average. Independent component analysis (ICA) was applied to identify and remove ocular, muscular, and cardiac artifacts. Full details of the preprocessing pipeline are provided in the Supplementary Methods.

4.6. Dynamic ACW-0

The auto-correlation window (ACW) is the standard method used to probe INTs [6,7,9]. The method is based on the computation of the signal's autocorrelation function (ACF), which is obtained correlating the signal with itself at increasing time lags.

Here, we computed the ACW-0, which is parametrized as the first time lag at which the temporal auto-correlation function (ACF) of the EEG time series reaches its zero value [3].

As we were interested in the dynamics of INTs, the ACW-0 was computed using a sliding-window approach [15] on all M/EEG datasets (window size = 8 s; step size = 10 %), resulting in a time series of 366 time points for each recording. A step size of 10 % represents a step of 800 ms.

These sliding window parameters, especially the window size, were chosen according to evidence that shows that dynamic connectivity measures, which are tightly related to INTs [47], show increased reliability when probed with sliding windows of a comparable duration [69,70].

4.7. k-means clustering

Our study leverages dynamic ACW-0 matrices derived from M/EEG data to extract recurring INT (Intrinsic Neural Timescale) topographic states using k-means++ clustering procedure: this is done in order to track the transitions between different INT topographies – i.e. INT state maps. A full overview of the methods used in this study is presented in the following paragraphs.

The k-means algorithm, a well-established unsupervised learning technique, is utilized to cluster data, aiming to partition input data into a predefined number (k) of distinct groups or clusters. After clustering, a low-dimensional representation of the data is obtained, assigning each observation (n) to a unique cluster k.

As we were interested in obtaining a discrete set of dynamic INT topographic states, we used MATLAB's *kmeans* function to partition dynamic ACW-0 (dACW-0) matrices into the most recurrent INT scalp distributions observed in our populations. First, the subjects' dynamic ACW-0 matrices were concatenated horizontally, to obtain a *channelsXwindows* matrix, which were then normalized (min-max feature scaling) before the clustering procedure. Consequently, the k-means++ algorithm ([71], pp. 1027–1035) was iteratively run 25 times, with ks ranging from 2 to 20. In fact, the k-means procedure can vary across iterations, since it starts by randomly assigning k centroids at each iteration; therefore, we ran each clustering procedure with 1000 repetitions times to avoid the influence of random seeding. Both squared Euclidian distance and cityblock (L1 distance) were used as distance metrics. As we didn't observe any significant difference between the two distance measures, we selected the latter to ensure consistence with previous literature.

The selection of the optimal number of INT maps rested on two different optimization criteria. In the first, the optimal number of maps consisted in finding the knee point of the k vs *within-cluster variance* graph - often referred to as the "elbow method" - which ensures an efficient compromise between the decrease of within-cluster variance and the simplicity. The second optimization criterion method used in this study is known as the Krzanowski-Lai criterion [72], which selects the optimal number of clusters based on a dispersion measure D.

Once the best number of clusters was selected, each INT sliding window was assigned as belonging to a state based on a competitive back-fitting procedure, similarly to Ref. [73]: first, each window was spatially correlated to all k map states, and then the state was assigned based on the highest spatial correlation value obtained. Please note that spatial correlation coefficients correspond directly to Pearson's correlation coefficients. This yielded, for each subject, a time series of the same temporal resolution of its original dACW-0 time series, representing the temporal succession of INT topographic states as a function of time.

4.8. Core-periphery organization

To probe for the presence of a degree of hierarchical organization in the MEG INT topographic states, parcel-level INT values were spatially correlated with a myelination index map, as in Ref. [39]. This map is obtained from HCP diffusion MRI (dMRI) data from over a thousand healthy individuals, and indexes the average density of T1w/T2w at each parcel. To ensure spatial correlation, the myelination map followed the same parcellation scheme (360 parcels) as the source-reconstructed MEG data.

To obtain a summary index of the core-periphery organization, parcels were further subdivided into the 12-networks categorization suggested in Ref. [11], and INT values averaged over all parcels belonging to the same network.

4.9. Runs test

A runs test [74] was used to decide whether the dynamic INT state time series were consistent with a random process. In this study, "runs" are defined as the number of consecutive data points either above or below the original time series' median value. This procedure determines whether the number of "runs" is lower than the number of runs expected in a random process, which allows to reject the null hypothesis of randomness, or equally high – in which case, the null hypothesis of randomness cannot be rejected. To obtain statistical significance for the runs test, we used MATLAB's *runstest* function.

4.10. Markov properties

Statistical properties of INT states transitions were investigated by modeling them as Markov Chains [75] and subsequently testing these models against 0^{th} and 1st order Markovianity. Testing against hypotheses yields knowledge about the temporal dependences in the states' time series: if the system under exam only holds memory of the previous state when transitioning into the current one, then its time series holds a property known as "Markovianity", and it can be reasonably modeled as a 1st order Markov Chain. If this property does not hold – current states do not depend on previous states – then we are observing a 0^{th} order Markov Chain.

First, the empirical transition matrix T was obtained. To statistically test for the 0^{th} and 1st Markov property, we used a log-likelihood ratio test, which compared the log-likelihood LL_m of the model order being tested and the log-likelihood LL_n at one order higher: for instance, to test for 0^{th} order Markovianity, 0^{th} and 1st order log-likelihoods were compared, 1st and 2nd order to test for 1st order Markovianity.

We assumed that the likelihood ratio test statistics followed a chi squared distribution with degrees of freedom *df*

$$df = (ns^m - ns^m) \times (ns - 1)$$

where ns is the number of states and m is the Markov order being tested. Consequently, p-values were defined as

$$p = 1 - (-2 \times (LL_m - LL_n)$$

with threshold for significance at $\alpha = 0.05$.

4.11. INT state transitions dynamics – Context-Tree Weighting and Sample Entropy

The degree of randomness (unpredictability) inherent in the time series describing transitions between INT states was first evaluated using the Context-Tree Weighting (CTW) compression algorithm [76,77], which provides a entropy estimator similar to that of the Lempel-Ziv Complexity [78], but with faster convergence and higher estimation accuracy on data with a low number of data points, offering higher accuracy and lower bias in entropy rate estimation. CTW is based on a variable-order Markov model, which hierarchically decomposes the symbol sequence into binary decisions and effectively captures long-range temporal dependencies in the data. This method is particularly well-suited for the aim of this study, as it is designed to operate on symbolized, discrete sequences—a natural fit for the discrete INT state transitions data. To this end, we used the MATLAB code implementation available at the github repository https://github.com/pmediano/EntRate.

Additionally, the unpredictability of the INT state transitions was further confirmed by computing the Sample Entropy (SampEn) [79] of the INT state transition time series. We used the SampEn function implemented in the open-source MATLAB toolbox *EntropyHub* [80]. SampEn estimates the log-likelihood that time series trends that are tightly related will remain similar in the following comparison, without allowing for self-counting. In computing SampEn, the parameter m denotes the embedding dimension, which represents the length of the trends – or "sequences" – to be compared; the parameter tau, instead, controls the time delay between points in a trend, which allows to capture temporal structures which go beyond the analysis of consecutive points, when tau is set at values higher than 1. Parameter choice for this study included: m = 3; tau = 1. Additionally, we used the suggested default *EntropyHub* radius threshold r (r = 0.2· σ, where σ is the standard deviation of the signal). The same parameters were used to estimate the complexity of the EEG signal (Supplementary Fig. 10).

4.12. Exponential decay fitting

The memory property of the dynamic INT state transition time series was probed in a series of steps. First, we computing a version of the autocorrelation function which suited better ordinal data: we pursued this aim by computing Cramer's V [81] on a copy of the signal at different time lags. The choice of Cramer's V, instead of the more classic ACF, was guided by the fact that the time series is composed of ordinal variables, and Pearson's correlation is only defined on continuous data.

The decay rate was obtained by fitting an exponential decay of the form

$$D = A \times e^{-dr \times x} + C$$

to the Cramer's V categorical autocorrelation time series (where *A* and *C* define the lower and upper bound of the fitted function, *dr* is the decay rate and *x* is the time lag). Since this function displayed an exponential decay only in its first portion, we performed the fitting procedure on a truncated version of the time series (until lag = 30). To fit the function to the data, the *curve_fit* function from the *scipy* Python library was used.

4.13. Statistics and reproducibility

Sample sizes of the M/EEG sample are indicated in section 4.1 and 4.4. Summary statistics of the dynamics of INT topographic states were indexed at both subject and group level and included the average state coverage (in percentages) - which describes the relative amount of time spent in one particular state with respect to the total duration of the recording - and the state transition matrix, describing the probability of transitioning from state to state (including self-transitions).

Spatial correlation between EEG scalp topographies was computed using Pearson correlation, after vectorizing the topographic maps, i.e., converting each 2D scalp distribution into a 1D column vector by stacking channel values. This is a widely adopted procedure in EEG research for comparing spatial configurations across conditions or states (e.g., in microstate and brain topography analyses) ([38], p. 20; [73]). To enhance the interpretability and robustness of statistical significance, we further conducted control analyses using Euclidean and cosine distance metrics, combined with a non-parametric bootstrap test (see Supplementary Methods 1.2 for details).

A spatial permutation "spin test" was applied to address the correspondence problem faced when correlating two cortical maps [82]. The spin test is a statistical approach for evaluating the significance of patterns of spatial relationships in brain imaging data: it works by iteratively projecting the spatial coordinates of the cortical maps onto a spherical surface, which is randomly rotated to reshuffle the spatial coordinates of the original maps' values. A null distribution is obtained by comparing the spin test correlation coefficients with the empirical coefficient. In this study, 1000 null models were generated and significance threshold was set at 5 %.

To correct for the family-wise error rate when performing multiple statistical tests, the Holm-Bonferroni method was applied.

To compare CTW and SampEn values at group level, we applied the non-parametric Wilcoxon rank-sum test with significance threshold at 5 %.

A chi-square test was performed on all EEG states to determine whether the groups differed significantly in their average durations.

The null hypothesis of equal means in the decay rate of the DoC sample was tested with the non-parametric Alexander-Govern approximation test. Post-hoc pairwise comparisons were performed with the Wilcoxon rank-sum test.

Effect sizes are reported with the η^2 metric for the non-parametric multivariate group comparisons, and with the z-statistic resulting from the Wilcoxon rank-sum test fon post-hoc pairwise comparisons.

To check for statistical significance on the group states' properties, the INT state time series were temporally scrambled iteratively (1000 repetitions each) to produce a test distribution: significance was set at $\alpha = 0.05$. Additionally, a surrogate test (100 repetitions each) was used to the same end (see Supplementary Methods 1.2).

CRediT authorship contribution statement

Andrea Buccellato: Writing – original draft, Visualization, Methodology, Investigation, Formal analysis, Conceptualization. **Di Zang:** Writing – original draft, Visualization, Formal analysis, Data curation, Conceptualization. **Yasir Çatal:** Writing – review & editing, Software, Data curation. **Bianca Ventura:** Writing – review & editing, Visualization. **Massimiliano Facca:** Software, Investigation. **Zengxin Qi:** Investigation. **Patrizia Bisiacchi:** Writing – review & editing, Supervision. **Alessandra Del Felice:** Writing – review & editing, Supervision. **Xuehai Wu:** Writing – review & editing, Writing – original draft, Supervision, Resources. **Georg Northoff:** Writing – review & editing, Writing – original draft, Supervision, Conceptualization.

Data, materials, and software availability

EEG data used in this study is subjected to sharing restrictions due to

privacy issues regarding sensitive clinical data. MATLAB (R2023a release) was used for this study. Most of the data analysis was conducted using the EEGLAB (http://sccn.ucsd.edu/eeglab/(accessed on June 6, 2023)) toolbox, an open-source MATLAB package and Python.

Ethics statement

Informed written consent before participation was obtained from all participants (or from their caregivers). This research was approved by the Ethical Committee of the Huashan Hospital of Fudan University (approval number HIRB-2014–281) and conducted in accordance with the Declaration of Helsinki guidelines.

Declaration of competing interest

The authors declare that they have no known competing financial interests or personal relationships that could have appeared to influence the work reported in this paper.

Acknowledgements and funding sources

This research has received funding from the European Union's Horizon 2020 Framework Program for Research and Innovation under the Specific Grant Agreement no, 785907 (Human Brain Project SGA2). Y.A. is grateful for the support by China Scholarship Council (202208510069). G.N. is grateful for funding provided by UMRF, uOBMRI, CIHR and PSI. We are also grateful to CIHR, NSERC, and SSHRC for supporting our tri-council grant from the Canada–UK Artificial Intelligence (AI) Initiative The self as agent–environment nexus: crossing disciplinary boundaries to help human selves and anticipate artificial selves' (ES/T01279X/1) (together with Karl J. Friston from the UK).

This work was also supported by the National Natural Science Foundation of China (Nos. 82271224); Shanghai Municipal Science and Technology Major Project (No.2018SHZDZX01), ZJ Lab, and Shanghai Center for Brain Science and Brain-Inspired Technology; SHANGHAI ZHOU LIANGFU MEDICAL DEVELOPMENT FOUNDATION "Brain Science and Brain Diseases Youth Innovation Program"; National High Level Hospital Clinical Research Funding (No. 2023-NHLHCRF-BQ-43).

ADF is supported by the following institutions: Italian Ministry of University and Research under the Italian PNRR (Piano Nazionale di Ripresa e Resilienza)funding scheme (Grant Number: MUR PE00000015); Italian Ministry of University and Research under the PRIN 2022 (Fondo per il Programma Nazionale di Ricerca e Progetti di Rilevante Interesse Nazionale) funding scheme. (Grant Number: 2022YPK5YB).

Appendix A. Supplementary data

Supplementary data to this article can be found online at https://doi.org/10.1016/j.compbiomed.2025.111102.

References

[1] S.B. Eickhoff, R.T. Constable, B.T.T. Yeo, Topographic organization of the cerebral cortex and brain cartography, Neuroimage 170 (2018) 332–347, https://doi.org/10.1016/j.neuroimage.2017.02.018.

[2] J.M. Huntenburg, P.-L. Bazin, D.S. Margulies, Large-scale gradients in human cortical organization, Trends Cognit. Sci. 22 (2018) 21–31, https://doi.org/10.1016/j.tics.2017.11.002.

[3] M. Golesorkhi, J. Gomez-Pilar, S. Tumati, M. Fraser, G. Northoff, Temporal hierarchy of intrinsic neural timescales converges with spatial core-periphery organization, Commun. Biol. 4 (2021) 277, https://doi.org/10.1038/s42003-021-01785-z.

[4] G. Northoff, P. Klar, M. Bein, A. Safron, As without, so within: how the brain's temporo-spatial alignment to the environment shapes consciousness, Interface Focus 13 (2023) 20220076, https://doi.org/10.1098/rsfs.2022.0076.

[5] D.S. Margulies, S.S. Ghosh, A. Goulas, M. Falkiewicz, J.M. Huntenburg, G. Langs, G. Bezgin, S.B. Eickhoff, F.X. Castellanos, M. Petrides, E. Jefferies, J. Smallwood, Situating the default-mode network along a principal gradient of macroscale cortical organization, Proc. Natl. Acad. Sci. USA 113 (2016) 12574–12579, https://doi.org/10.1073/pnas.1608282113.

[6] M. Golesorkhi, J. Gomez-Pilar, F. Zilio, N. Berberian, A. Wolff, M.C.E. Yagoub, G. Northoff, The brain and its time: intrinsic neural timescales are key for input processing, Commun. Biol. 4 (2021) 970, https://doi.org/10.1038/s42003-021-02483-6.

[7] A. Wolff, N. Berberian, M. Golesorkhi, J. Gomez-Pilar, F. Zilio, G. Northoff, Intrinsic neural timescales: temporal integration and segregation, Trends Cognit. Sci. 26 (2022) 159–173, https://doi.org/10.1016/j.tics.2021.11.007.

[8] M. Demirtaş, J.B. Burt, M. Helmer, J.L. Ji, B.D. Adkinson, M.F. Glasser, D.C. Van Essen, S.N. Sotiropoulos, A. Anticevic, J.D. Murray, Hierarchical heterogeneity across human cortex shapes large-scale neural dynamics, Neuron 101 (2019) 1181–1194.e13, https://doi.org/10.1016/j.neuron.2019.01.017.

[9] C.J. Honey, T. Thesen, T.H. Donner, L.J. Silbert, C.E. Carlson, O. Devinsky, W. K. Doyle, N. Rubin, D.J. Heeger, U. Hasson, Slow cortical dynamics and the accumulation of information over long timescales, Neuron 76 (2012) 423–434, https://doi.org/10.1016/j.neuron.2012.08.011.

[10] J.D. Murray, A. Bernacchia, D.J. Freedman, R. Romo, J.D. Wallis, X. Cai, C. Padoa-Schioppa, T. Pasternak, H. Seo, D. Lee, X.-J. Wang, A hierarchy of intrinsic timescales across primate cortex, Nat. Neurosci. 17 (2014) 1661–1663, https://doi.org/10.1038/nn.3862.

[11] T. Ito, L.J. Hearne, M.W. Cole, A cortical hierarchy of localized and distributed processes revealed via dissociation of task activations, connectivity changes, and intrinsic timescales, Neuroimage 221 (2020) 117141, https://doi.org/10.1016/j.neuroimage.2020.117141.

[12] R.V. Raut, A.Z. Snyder, M.E. Raichle, Hierarchical dynamics as a macroscopic organizing principle of the human brain, Proc. Natl. Acad. Sci. USA 117 (2020) 20890–20897, https://doi.org/10.1073/pnas.2003383117.

[13] P. Klar, Y. Çatal, S. Fogel, G. Jocham, R. Langner, A.M. Owen, G. Northoff, Auditory inputs modulate intrinsic neuronal timescales during sleep, Commun. Biol. 6 (2023) 1180, https://doi.org/10.1038/s42003-023-05566-8.

[14] A. Wolman, Y. Çatal, A. Wolff, S. Wainio-Theberge, A. Scalabrini, A.E. Ahmadi, G. Northoff, Intrinsic neural timescales mediate the cognitive bias of self – temporal integration as key mechanism, Neuroimage 268 (2023) 119896, https://doi.org/10.1016/j.neuroimage.2023.119896.

[15] S. Lechner, G. Northoff, Prolonged intrinsic neural timescales dissociate from phase coherence in schizophrenia, Brain Sci. 13 (2023) 695, https://doi.org/10.3390/brainsci13040695.

[16] J.A. Hartigan, M.A. Wong, Algorithm AS 136: a K-Means clustering algorithm, Applied Statistics 28 (1979) 100, https://doi.org/10.2307/2346830.

[17] F. Cavanna, M.G. Vilas, M. Palmucci, E. Tagliazucchi, Dynamic functional connectivity and brain metastability during altered states of consciousness, Neuroimage 180 (2018) 383–395, https://doi.org/10.1016/j.neuroimage.2017.09.065.

[18] M.E. Raichle, The brain's default mode network, Annu. Rev. Neurosci. 38 (2015) 433–447, https://doi.org/10.1146/annurev-neuro-071013-014030.

[19] J. Britz, D. Van De Ville, C.M. Michel, BOLD correlates of EEG topography reveal rapid resting-state network dynamics, Neuroimage 52 (2010) 1162–1170, https://doi.org/10.1016/j.neuroimage.2010.02.052.

[20] J. Cabral, M.L. Kringelbach, G. Deco, Functional connectivity dynamically evolves on multiple time-scales over a static structural connectome: models and mechanisms, Neuroimage 160 (2017) 84–96, https://doi.org/10.1016/j.neuroimage.2017.03.045.

[21] X. Di, B.B. Biswal, Dynamic brain functional connectivity modulated by resting-state networks, Brain Struct. Funct. 220 (2015) 37–46, https://doi.org/10.1007/s00429-013-0634-3.

[22] H.-J. Park, K. Friston, Structural and functional brain networks: from connections to cognition, Science 342 (2013) 1238411, https://doi.org/10.1126/science.1238411.

[23] E. Tagliazucchi, F. Von Wegner, A. Morzelewski, V. Brodbeck, H. Laufs, Dynamic BOLD functional connectivity in humans and its electrophysiological correlates, Front. Hum. Neurosci. 6 (2012), https://doi.org/10.3389/fnhum.2012.00339.

[24] D. Li, P.E. Vlisides, G.A. Mashour, Dynamic reconfiguration of frequency-specific cortical coactivation patterns during psychedelic and anesthetized states induced by ketamine, Neuroimage 249 (2022) 118891, https://doi.org/10.1016/j.neuroimage.2022.118891.

[25] E.P. Hoel, L. Albantakis, W. Marshall, G. Tononi, Can the macro beat the micro? Integrated information across spatiotemporal scales, Neurosci Conscious 2016 (2016) niw012, https://doi.org/10.1093/nc/niw012.

[26] D.C. Van Essen, S.M. Smith, D.M. Barch, T.E.J. Behrens, E. Yacoub, K. Ugurbil, The WU-Minn human connectome project: an overview, Neuroimage 80 (2013) 62–79, https://doi.org/10.1016/j.neuroimage.2013.05.041.

[27] J.T. Giacino, J.J. Fins, S. Laureys, N.D. Schiff, Disorders of consciousness after acquired brain injury: the state of the science, Nat. Rev. Neurol. 10 (2014) 99–114, https://doi.org/10.1038/nrneurol.2013.279.

[28] T. Bayne, J. Hohwy, A.M. Owen, Are there levels of consciousness? Trends Cognit. Sci. 20 (2016) 405–413, https://doi.org/10.1016/j.tics.2016.03.009.

[29] K. Golden, Y.G. Bodien, J.T. Giacino, Disorders of consciousness, Phys. Med. Rehabil. Clin 35 (2024) 15–33, https://doi.org/10.1016/j.pmr.2023.06.011.

[30] the European Task Force on Disorders of Consciousness, S. Laureys, G.G. Celesia, F. Cohadon, J. Lavrijsen, J. León-Carrión, W.G. Sannita, L. Sazbon, E. Schmutzhard, K.R. Von Wild, A. Zeman, G. Dolce, Unresponsive wakefulness syndrome: a new name for the vegetative state or apallic syndrome, BMC Med. 8 (2010) 68, https://doi.org/10.1186/1741-7015-8-68.

[31] J.T. Giacino, S. Ashwal, N. Childs, R. Cranford, B. Jennett, D.I. Katz, J.P. Kelly, J. H. Rosenberg, J. Whyte, R.D. Zafonte, N.D. Zasler, The minimally conscious state: definition and diagnostic criteria, Neurology 58 (2002) 349–353, https://doi.org/10.1212/WNL.58.3.349.
[32] G. Northoff, Z. Huang, How do the brain's time and space mediate consciousness and its different dimensions? temporo-spatial theory of consciousness (TTC), Neurosci. Biobehav. Rev. 80 (2017) 630–645, https://doi.org/10.1016/j.neubiorev.2017.07.013.
[33] G. Northoff, F. Zilio, Temporo-spatial theory of consciousness (TTC) – bridging the gap of neuronal activity and phenomenal states, Behav. Brain Res. 424 (2022) 113788, https://doi.org/10.1016/j.bbr.2022.113788.
[34] F. Von Wegner, E. Tagliazucchi, H. Laufs, Information-theoretical analysis of resting state EEG microstate sequences - non-markovianity, non-stationarity and periodicities, Neuroimage 158 (2017) 99–111, https://doi.org/10.1016/j.neuroimage.2017.06.062.
[35] J. Chen, U. Hasson, C.J. Honey, Processing timescales as an organizing principle for primate cortex, Neuron 88 (2015) 244–246, https://doi.org/10.1016/j.neuron.2015.10.010.
[36] U. Hasson, E. Yang, I. Vallines, D.J. Heeger, N. Rubin, A hierarchy of temporal receptive windows in human cortex, J. Neurosci. 28 (2008) 2539–2550, https://doi.org/10.1523/JNEUROSCI.5487-07.2008.
[37] F. Zilio, J. Gomez-Pilar, S. Cao, J. Zhang, D. Zang, Z. Qi, J. Tan, T. Hiromi, X. Wu, S. Fogel, Z. Huang, M.R. Hohmann, T. Fomina, M. Synofzik, M. Grosse-Wentrup, A. M. Owen, G. Northoff, Are intrinsic neural timescales related to sensory processing? Evidence from abnormal behavioral states, Neuroimage 226 (2021) 117579, https://doi.org/10.1016/j.neuroimage.2020.117579.
[38] C.M. Michel, T. Koenig, EEG microstates as a tool for studying the temporal dynamics of whole-brain neuronal networks: a review, Neuroimage 180 (2018) 577–593, https://doi.org/10.1016/j.neuroimage.2017.11.062.
[39] B.Q. Rosen, E. Halgren, A whole-cortex probabilistic diffusion tractography connectome, eNeuro 8 (2021) 416–420, https://doi.org/10.1523/ENEURO.0416-20.2020, 2020.
[40] J.B. Burt, M. Demirtaş, W.J. Eckner, N.M. Navejar, J.L. Ji, W.J. Martin, A. Bernacchia, A. Anticevic, J.D. Murray, Hierarchy of transcriptomic specialization across human cortex captured by structural neuroimaging topography, Nat. Neurosci. 21 (2018) 1251–1259, https://doi.org/10.1038/s41593-018-0195-0.
[41] P. Fotiadis, M. Cieslak, X. He, L. Caciagli, M. Ouellet, T.D. Satterthwaite, R. T. Shinohara, D.S. Bassett, Myelination and excitation-inhibition balance synergistically shape structure-function coupling across the human cortex, Nat. Commun. 14 (2023) 6115, https://doi.org/10.1038/s41467-023-41686-9.
[42] D. Wu, L. Fan, M. Song, H. Wang, C. Chu, S. Yu, T. Jiang, Hierarchy of connectivity–function relationship of the human cortex revealed through predicting activity across functional domains, Cerebr. Cortex 30 (2020) 4607–4616, https://doi.org/10.1093/cercor/bhaa063.
[43] C. Chatfield, The Analysis of Time Series, 0 ed., Chapman and Hall/CRC, 2003 https://doi.org/10.4324/9780203491683.
[44] N. Brake, F. Duc, A. Rokos, F. Arseneau, S. Shahiri, A. Khadra, G. Plourde, A neurophysiological basis for aperiodic EEG and the background spectral trend, Nat. Commun. 15 (2024) 1514, https://doi.org/10.1038/s41467-024-45922-8.
[45] M. Murphy, R. Stickgold, D. Öngür, Electroencephalogram microstate abnormalities in early-course psychosis, Biol. Psychiatry Cogn. Neurosci. Neuroimaging 5 (2020) 35–44, https://doi.org/10.1016/j.bpsc.2019.07.006.
[46] P. Sorrentino, G. Rabuffo, F. Baselice, E. Troisi Lopez, M. Liparoti, M. Quarantelli, G. Sorrentino, C. Bernard, V. Jirsa, Dynamical interactions reconfigure the gradient of cortical timescales, Network Neurosci. 7 (2023) 73–85, https://doi.org/10.1162/netn_a_00270.
[47] R. Chaudhuri, K. Knoblauch, M.-A. Gariel, H. Kennedy, X.-J. Wang, A large-scale circuit mechanism for hierarchical dynamical processing in the primate cortex, Neuron 88 (2015) 419–431, https://doi.org/10.1016/j.neuron.2015.09.008.
[48] G. Rabuffo, P. Sorrentino, C. Bernard, V. Jirsa, Spontaneous neuronal avalanches as a correlate of access consciousness, Front. Psychol. 13 (2022) 1008407, https://doi.org/10.3389/fpsyg.2022.1008407.
[49] L. Albantakis, L. Barbosa, G. Findlay, M. Grasso, A.M. Haun, W. Marshall, W.G. P. Mayner, A. Zaeemzadeh, M. Boly, B.E. Juel, S. Sasai, K. Fujii, I. David, J. Hendren, J.P. Lang, G. Tononi, Integrated information theory (IIT) 4.0: formulating the properties of phenomenal existence in physical terms, PLoS Comput. Biol. 19 (2023) e1011465, https://doi.org/10.1371/journal.pcbi.1011465.
[50] R.L. Carhart-Harris, The entropic brain - revisited, Neuropharmacology 142 (2018) 167–178, https://doi.org/10.1016/j.neuropharm.2018.03.010.
[51] J. Wang, X. Hu, Z. Hu, Z. Sun, S. Laureys, H. Di, The misdiagnosis of prolonged disorders of consciousness by a clinical consensus compared with repeated coma-recovery scale-revised assessment, BMC Neurol. 20 (2020) 343, https://doi.org/10.1186/s12883-020-01924-9.
[52] S. Sarasso, A.G. Casali, S. Casarotto, M. Rosanova, C. Sinigaglia, M. Massimini, Consciousness and complexity: a consilience of evidence, Neurosci. Consciousness (2021), https://doi.org/10.1093/nc/niab023, 2021, niab023.
[53] M.M. Monti, A. Vanhaudenhuyse, M.R. Coleman, M. Boly, J.D. Pickard, L. Tshibanda, A.M. Owen, S. Laureys, Willful modulation of brain activity in disorders of consciousness, N. Engl. J. Med. 362 (2010) 579–589, https://doi.org/10.1056/NEJMoa0905370.
[54] C. Schnakers, C. Bauer, R. Formisano, E. Noé, R. Llorens, N. Lejeune, M. Farisco, L. Teixeira, A.-M. Morrissey, S. De Marco, V. Veeramuthu, K. Ilina, B.L. Edlow, O. Gosseries, M. Zandalasini, F. De Bellis, A. Thibaut, A. Estraneo, What names for covert awareness? A systematic review, Front. Hum. Neurosci. 16 (2022) 971315, https://doi.org/10.3389/fnhum.2022.971315.
[55] J. Frohlich, J.S. Crone, P.A.M. Mediano, D. Toker, D. Bor, Editorial: dissociations between neural activity and conscious state: a key to understanding consciousness, Front. Hum. Neurosci. 17 (2023) 1256168, https://doi.org/10.3389/fnhum.2023.1256168.
[56] K.D. Himberger, H.-Y. Chien, C.J. Honey, Principles of temporal processing across the cortical hierarchy, Neuroscience 389 (2018) 161–174, https://doi.org/10.1016/j.neuroscience.2018.04.030.
[57] T.O. Laumann, A.Z. Snyder, A. Mitra, E.M. Gordon, C. Gratton, B. Adeyemo, A. W. Gilmore, S.M. Nelson, J.J. Berg, D.J. Greene, J.E. McCarthy, E. Tagliazucchi, H. Laufs, B.L. Schlaggar, N.U.F. Dosenbach, S.E. Petersen, On the stability of BOLD fMRI correlations, Cereb. Cortex cercor (2016), https://doi.org/10.1093/cercor/bhw265 bhw265v1.
[58] D.J. Lurie, D. Kessler, D.S. Bassett, R.F. Betzel, M. Breakspear, S. Kheilholz, A. Kucyi, R. Liégeois, M.A. Lindquist, A.R. McIntosh, R.A. Poldrack, J.M. Shine, W. H. Thompson, N.Z. Bielczyk, L. Douw, D. Kraft, R.L. Miller, M. Muthuraman, L. Pasquini, A. Razi, D. Vidaurre, H. Xie, V.D. Calhoun, Questions and controversies in the study of time-varying functional connectivity in resting fMRI, Network Neurosci. 4 (2020) 30–69, https://doi.org/10.1162/netn_a_00116.
[59] R. Liégeois, J. Li, R. Kong, C. Orban, D. Van De Ville, T. Ge, M.R. Sabuncu, B.T. T. Yeo, Resting brain dynamics at different timescales capture distinct aspects of human behavior, Nat. Commun. 10 (2019) 2317, https://doi.org/10.1038/s41467-019-10317-7.
[60] J. Vorwerk, C.H. Wolters, D. Baumgarten, Global sensitivity of EEG source analysis to tissue conductivity uncertainties, Front. Hum. Neurosci. 18 (2024) 1335212, https://doi.org/10.3389/fnhum.2024.1335212.
[61] J. Rizkallah, J. Annen, J. Modolo, O. Gosseries, P. Benquet, S. Mortaheb, H. Amoud, H. Cassol, A. Mheich, A. Thibaut, C. Chatelle, M. Hassan, R. Panda, F. Wendling, S. Laureys, Decreased integration of EEG source-space networks in disorders of consciousness, Neuroimage: Clinical 23 (2019) 101841, https://doi.org/10.1016/j.nicl.2019.101841.
[62] A.E. Cathignol, L. Kusch, M. Angiolelli, E.T. Lopez, A. Polverino, A. Romano, G. Sorrentino, V. Jirsa, G. Rabuffo, P. Sorrentino, Magnetoencephalography dimensionality reduction informed by dynamic brain states, Eur. J. Neurosci. 61 (2025) e70128, https://doi.org/10.1111/ejn.70128.
[63] L.J. Larson-Prior, R. Oostenveld, S. Della Penna, G. Michalareas, F. Prior, A. Babajani-Feremi, J.-M. Schoffelen, L. Marzetti, F. De Pasquale, F. Di Pompeo, J. Stout, M. Woolrich, Q. Luo, R. Bucholz, P. Fries, V. Pizzella, G.L. Romani, M. Corbetta, A.Z. Snyder, Adding dynamics to the human connectome project with MEG, Neuroimage 80 (2013) 190–201, https://doi.org/10.1016/j.neuroimage.2013.05.056.
[64] D.C. Van Essen, K. Ugurbil, E. Auerbach, D. Barch, T.E.J. Behrens, R. Bucholz, A. Chang, L. Chen, M. Corbetta, S.W. Curtiss, S. Della Penna, D. Feinberg, M. F. Glasser, N. Harel, A.C. Heath, L. Larson-Prior, D. Marcus, G. Michalareas, S. Moeller, R. Oostenveld, S.E. Petersen, F. Prior, B.L. Schlaggar, S.M. Smith, A. Z. Snyder, J. Xu, E. Yacoub, The human connectome project: a data acquisition perspective, Neuroimage 62 (2012) 2222–2231, https://doi.org/10.1016/j.neuroimage.2012.02.018.
[65] M.F. Glasser, T.S. Coalson, E.C. Robinson, C.D. Hacker, J. Harwell, E. Yacoub, K. Ugurbil, J. Andersson, C.F. Beckmann, M. Jenkinson, S.M. Smith, D.C. Van Essen, A multi-modal parcellation of human cerebral cortex, Nature 536 (2016) 171–178, https://doi.org/10.1038/nature18933.
[66] J.T. Giacino, K. Kalmar, J. Whyte, The JFK coma recovery scale-revised: measurement characteristics and diagnostic utility11No commercial party having a direct financial interest in the results of the research supporting this article has or will confer a benefit upon the authors or upon any organization with which the authors are associated, Arch. Phys. Med. Rehabil. 85 (2004) 2020–2029, https://doi.org/10.1016/j.apmr.2004.02.033.
[67] G. Teasdale, B. Jennett, Assessment of coma and impaired consciousness, Lancet 304 (1974) 81–84, https://doi.org/10.1016/S0140-6736(74)91639-0.
[68] A. Delorme, S. Makeig, EEGLAB: an open source toolbox for analysis of single-trial EEG dynamics including independent component analysis, J. Neurosci. Methods 134 (2004) 9–21, https://doi.org/10.1016/j.jneumeth.2003.10.009.
[69] M. Fraschini, M. Demuru, A. Crobe, F. Marrosu, C.J. Stam, A. Hillebrand, The effect of epoch length on estimated EEG functional connectivity and brain network organisation, J. Neural. Eng. 13 (2016) 036015, https://doi.org/10.1088/1741-2560/13/3/036015.
[70] Pierpaolo Sorrentino, E. Troisi Lopez, A. Romano, C. Granata, M.C. Corsi, G. Sorrentino, V. Jirsa, Brain fingerprint is based on the aperiodic, scale-free, neuronal activity, Neuroimage 277 (2023) 120260, https://doi.org/10.1016/j.neuroimage.2023.120260.
[71] Association for Computing Machinery, Society for Industrial and Applied Mathematics, in: Proceedings of the Eighteenth Annual ACM-SIAM Symposium on Discrete Algorithms: New Orleans, La., January 7 - 9, 2007. Presented at the Symposium on Discrete Algorithms, Association for Computing Machinery, New York, NY, 2007 [u.a.].
[72] W.J. Krzanowski, Y.T. Lai, A criterion for determining the number of groups in a data set using sum-of-squares clustering, Biometrics 44 (1988) 23, https://doi.org/10.2307/2531893.
[73] M.M. Murray, D. Brunet, C.M. Michel, Topographic ERP analyses: a step-by-step tutorial review, Brain Topogr. 20 (2008) 249–264, https://doi.org/10.1007/s10548-008-0054-5.
[74] J.V. Bradley, DISTRIBUTION-FREE STATISTICAL TESTS, Defense Technical Information Center, Fort Belvoir, VA, 1960, https://doi.org/10.21236/AD0249268.

[75] P.A. Gagniuc, Markov Chains: from Theory to Implementation and Experimentation, John Wiley & Sons, Hoboken, NJ, 2017.
[76] R. Begleiter, R. El-Yaniv, G. Yona, On prediction using variable order markov models. https://doi.org/10.48550/ARXIV.1107.0051, 2011.
[77] P.A.M. Mediano, F.E. Rosas, C. Timmermann, L. Roseman, D.J. Nutt, A. Feilding, M. Kaelen, M.L. Kringelbach, A.B. Barrett, A.K. Seth, S. Muthukumaraswamy, D. Bor, R.L. Carhart-Harris, Effects of external stimulation on psychedelic state neurodynamics, ACS Chem. Neurosci. 15 (2024) 462–471, https://doi.org/10.1021/acschemneuro.3c00289.
[78] J. Ziv, A. Lempel, A universal algorithm for sequential data compression, IEEE Trans. Inf. Theor. 23 (1977) 337–343, https://doi.org/10.1109/TIT.1977.1055714.
[79] J.S. Richman, J.R. Moorman, Physiological time-series analysis using approximate entropy and sample entropy, Am. J. Physiol. Heart Circ. Physiol. 278 (2000) H2039–H2049, https://doi.org/10.1152/ajpheart.2000.278.6.H2039.
[80] M.W. Flood, B. Grimm, EntropyHub: an open-source toolkit for entropic time series analysis, PLoS One 16 (2021) e0259448, https://doi.org/10.1371/journal.pone.0259448.
[81] W. Bergsma, A bias-correction for Cramér's and Tschuprow's, J. Korean Surg. Soc. 42 (2013) 323–328, https://doi.org/10.1016/j.jkss.2012.10.002.
[82] A.F. Alexander-Bloch, H. Shou, S. Liu, T.D. Satterthwaite, D.C. Glahn, R. T. Shinohara, S.N. Vandekar, A. Raznahan, On testing for spatial correspondence between maps of human brain structure and function, Neuroimage 178 (2018) 540–551, https://doi.org/10.1016/j.neuroimage.2018.05.070.